⌘ *Author's Choice*

THE JOURNAL OF BIOLOGICAL CHEMISTRY VOL. 285, NO. 17, pp. 12979–12989, April 23, 2010

Regulation of Inositol 1,4,5-Trisphosphate Receptors by cAMP Independent of cAMP-dependent Protein Kinase*[S]

Received for publication, December 17, 2009, and in revised form, February 11, 2010 Published, JBC Papers in Press, February 26, 2010, DOI 10.1074/jbc.M109.096016

Stephen C. Tovey, Skarlatos G. Dedos, Taufiq Rahman[1], Emily J. A. Taylor, Evangelia Pantazaka, and Colin W. Taylor[2]

From the Department of Pharmacology, University of Cambridge, Tennis Court Road, Cambridge CB2 1PD, United Kingdom

In HEK cells stably expressing type 1 receptors for parathyroid hormone (PTH), PTH causes a sensitization of inositol 1,4,5-trisphosphate receptors (IP_3R) to IP_3 that is entirely mediated by cAMP and requires cAMP to pass directly from type 6 adenylyl cyclase (AC6) to IP_3R2. Using DT40 cells expressing single subtypes of mammalian IP_3R, we demonstrate that high concentrations of cAMP similarly sensitize all IP_3R isoforms to IP_3 by a mechanism that does not require cAMP-dependent protein kinase (PKA). IP_3 binding to IP_3R2 is unaffected by cAMP, and sensitization is not mediated by the site through which ATP potentiates responses to IP_3. In single channel recordings from excised nuclear patches of cells expressing IP_3R2, cAMP alone had no effect, but it increased the open probability of IP_3R2 activated by a submaximal concentration of IP_3 alone or in combination with a maximally effective concentration of ATP. These results establish that cAMP itself increases the sensitivity of all IP_3R subtypes to IP_3. For IP_3R2, this sensitization results from cAMP binding to a novel site that increases the efficacy of IP_3. Using stably expressed short hairpin RNA to reduce expression of the G-protein, $G\alpha_s$, we demonstrate that attenuation of AC activity by loss of $G\alpha_s$ more substantially reduces sensitization of IP_3R by PTH than does comparable direct inhibition of AC. This suggests that $G\alpha_s$ may also specifically associate with each AC·IP_3R complex. We conclude that all three subtypes of IP_3R are regulated by cAMP independent of PKA. In HEK cells, where IP_3R2 selectively associates with AC6, $G\alpha_s$ also associates with the AC·IP_3R signaling junction.

Ca^{2+} and cAMP are two of a limited number of intracellular messengers used by cells to regulate a diverse array of cellular events in response to many different extracellular stimuli. The specificity of these messengers is provided by the spatio-temporal organization of their concentration changes within cells (1–4) and by complex interactions between them (2, 5, 6). In addressing the means whereby parathyroid hormone (PTH)[3] regulates release of Ca^{2+} from intracellular stores, we have shown that PTH acts entirely via cAMP to increase the sensitivity of IP_3 receptors (IP_3R) to IP_3, thereby potentiating the Ca^{2+} signals evoked by other receptors that stimulate IP_3 formation (7). This effect of PTH is not mediated by the common targets of cAMP, PKA, and exchange proteins activated by cAMP (epac), but results instead from cAMP binding directly to a low affinity site on either the IP_3R itself or a protein tightly associated with it (7). These results identify the IP_3R as a new target for regulation by cAMP and so reveal another site at which cAMP and Ca^{2+} signaling pathways interact. The results also highlighted the importance of the precise spatial relationship between adenylyl cyclase (AC) and IP_3R, because cAMP appears to pass directly and selectively from type 6 AC (AC6) to the type 2 IP_3R (IP_3R2) via an association that we termed an AC·IP_3R junction (7) (Fig. 1*A*).

These observations led us to define two forms of local cAMP signaling (Fig. 1*A*). The first mode, represented by the AC·IP_3R junction, is binary signaling. Here, cAMP is delivered directly to its target at very high concentrations by a closely associated AC; cAMP then switches the target on in all-or-nothing fashion. The second mode is analog signaling, where targets further away from AC, like PKA and exchange proteins activated by cAMP, respond to graded changes in cAMP concentration. The low affinity of the IP_3R for cAMP ensures that diffusion of cAMP is probably sufficient to terminate a response and insulate one junction from its neighbors. For analog signaling, local degradation of cAMP by associated cyclic nucleotide phosphodiesterases is required to terminate the response and maintain the spatial organization of cAMP signaling (Fig. 1*A*) (7, 8).

Here, we address two further questions related to cAMP signaling to IP_3R. First, although we have shown that, in intact HEK cells the effects of PTH are selectively mediated by IP_3R2, it is unclear whether this results solely from a selective association of IP_3R2 with AC6, or whether IP_3R2 is also unique among the three IP_3R subtypes in responding to cAMP. We demonstrate, using IP_3R1–3 expressed in DT40 cells lacking native IP_3R, that all IP_3R subtypes are regulated by cAMP itself. Second, although AC6 and IP_3R2 are associated in a signaling

* This work was supported in part by The Wellcome Trust (Grant 085295), the Medical Research Council, UK (Grant G0700843), and the Biotechnology and Biological Sciences Research Council, UK (Grant BB/E004660/1).

⌘ *Author's Choice*—Final version full access.

[S] The on-line version of this article (available at http://www.jbc.org) contains supplemental Fig. S1, Table S1 and supplemental Experimental Procedures, Discussion, and an additional reference.

[1] A Drapers' research fellow at Pembroke College, Cambridge.

[2] To whom correspondence should be addressed. Tel./Fax: 44-1223-334058; E-mail: cwt1000@cam.ac.uk.

[3] The abbreviations used are: PTH, residues 1–34 of human parathyroid hormone; AC, adenylyl cyclase; AC6, type 6 adenylyl cyclase; B_{max}, maximal concentration of binding sites; $[Ca^{2+}]_i$, intracellular free Ca^{2+} concentration; CCh, carbamylcholine chloride; CLM, cytosol-like medium; DDA, 2′,5′-dideoxyadenosine; EC_{50}, half-maximally effective concentration; H89, *N*-[2-((*p*-bromocinnamyl)amino)ethyl]-5-isoquinoline sulfonamide; HBS, HEPES-buffered saline; HEK-PR1 (HEK-PR1α_s^-), human embryonic kidney cells stably expressing human type 1 PTH receptor (and also stably expressing shRNA for α_s); IP_3, inositol 1,4,5-trisphosphate; IP_3R, IP_3 receptor; ORF, open reading frame; PKA, protein kinase A (cAMP-dependent protein kinase); PS, pipette solution; shRNA, short hairpin RNA; SQ 22536, 9-(tetrahydro-2′-furyl)adenine; SQ/DDA, 1 mM SQ 22536 with 200 μM DDA (used to inhibit AC); BAPTA, 1,2-bis(2-aminophenoxy)ethane-*N*,*N*,*N*′,*N*′-tetraacetic acid; ATPB, B binding site for ATP in IP_3R2.

complex (the AC6·IP_3R2 junction, Fig. 1*A*), it is unclear whether other components of the signaling pathway linking PTH receptors to sensitization of IP_3R are also uniquely associated with individual AC6·IP_3R junctions. By selectively inhibiting $G\alpha_s$ expression using stably expressed shRNA, we demonstrate that $G\alpha_s$ is probably also specifically associated with AC·IP_3R junctions.

EXPERIMENTAL PROCEDURES

Cells and Vectors—HEK 293 cells stably transfected with human type 1 PTH receptor (HEK-PR1 cells) were cultured as described (9). A modified pSUPER vector (10) was used for shRNA-mediated knockdown of $G\alpha_s$ in HEK-PR1 cells. An expression cassette for blasticidin resistance from pcDNA6/TR (Invitrogen) was cloned upstream of the polymerase-III H1-RNA promoter of pSUPER to generate a pSUPERBlank vector. Primers 1 and 2 for human $G\alpha_s$ (see supplemental Table S1 for primer sequences) were annealed, phosphorylated by T4 polynucleotide kinase (New England Biolabs), and ligated into the BglII-HindIII sites of pSUPERBlank to create the pSUPER$G\alpha_s$ vector. The plasmids, pSUPERBlank and pSUPER$G\alpha_s$, were linearized and transfected into HEK-PR1 cells (5 μg of DNA/10^6 cells) using Transfast™ Reagent (Promega). Transfected cells were selected using blasticidin (10 μg/ml) and G418 (800 μg/ml). Clonally isolated cells were screened for $G\alpha_s$ by immunoblotting using a $G\alpha_s$ antiserum (RM/1, 1:1000, New England Nuclear). Appropriate clones were further propagated for use in assays of cAMP and $[Ca^{2+}]_i$.

DT40 cells in which each IP_3R gene had been disrupted (DT40KO cells) (11) were cultured as described (12). The ORF of rat IP_3R1 (GenBank™ accession number GQ233032.1) was amplified by PCR from the expression vector pCMVI-9-IP_3R1 (13) using primers 3 and 4 (supplemental Table S1), and cloned as an EcoRI fragment into pENTR1a vector (Invitrogen). The ORF of mouse IP_3R2 (GenBank™ accession number AB182290) was amplified by PCR as two fragments from the expression vector pcDNA3-IP_3R2 (14). The 5′ fragment (1–3297) was amplified by PCR using primers 5 and 6 and cloned as a SalI-XhoI fragment into pENTR1a. Then the entire ORF (1–8196) was amplified by PCR using primers 5 and 7, digested with KpnI and XhoI, and the resulting fragment (2230–8196) was cloned into pENTR1a. Finally, a SalI-BstBI fragment (1–2711) from the first construct was cloned into the second construct (replacing the smaller SalI-BstBI fragment) to give the entire ORF (1–8196) of mouse IP_3R2 in pENTR1a. Supplemental Experimental Procedures provide further details of the cloning and expression of IP_3R2. The ORF of rat IP_3R3 (GenBank™ accession number GQ233031.1) was amplified by PCR from the expression vector pCB6-IP_3R3 (15) using primers 8 and 9, and cloned as an EcoRI fragment into pENTR1a vector (Invitrogen). Each pENTR1a-IP_3R construct was recombined with pcDNA3.2/V5-DEST (Invitrogen) to generate the Gateway-compatible expression vectors pcDNA3.2-IP_3R1 (2 and 3). DT40KO cells were transfected by nucleofection with linearized constructs of pcDNA3.2-IP_3R1 (2 or 3) using solution T and program B23 (Amaxa) using 5 μg of DNA/10^6 cells. G418 (2 mg/ml) was used to select and amplify clones of cells. Expression of IP_3R in each cell line was quantified by immunoblotting using an anti-peptide antiserum (AbC (16)) that interacts equally with all three IP_3R subtypes. GeneTools (Syngene) was used to quantify band intensities on immunoblots. To estimate numbers of IP_3R in each DT40 cell line, immunoblots were calibrated using membranes prepared from rat cerebellum in which the receptor density (B_{max}) had been measured by equilibrium competition [^{3}H]IP_3 binding.

For expression of mouse IP_3R2 in Sf9 cells, pENTR1a-IP_3R2 was recombined with Gateway-compatible BaculoDirect C-Term linear DNA (Invitrogen) to generate a recombinant baculovirus using the BaculoDirect™ C-Term expression kit (Invitrogen). Sf9 cells were cultured as previously described (17), they were then infected with the recombinant virus DNA, and the virus was isolated according to the manufacturer's instructions (Invitrogen). For IP_3R2 expression, cells were infected at a multiplicity of infection of 10.

Measurements of IP_3-evoked Ca^{2+} Release from Permeabilized Cells—The intracellular stores of DT40 cells stably expressing mammalian IP_3R were loaded with Mag-fluo-4 to allow measurement of the luminal-free [Ca^{2+}] (12). Cells were then permeabilized by incubation with saponin (10 μg/ml) and immobilized in 96-well plates to allow continuous monitoring of the Ca^{2+} content of the intracellular stores using a FlexStation fluorescence plate reader (MDS Analytical Devices) (12). All experiments were performed at 20 °C in cytosol-like medium with a free [Ca^{2+}] of 220 nM (CLM: 140 mM KCl, 20 mM NaCl, 1 mM EGTA, 375 μM $CaCl_2$, 20 mM Pipes, pH 7.0). MgATP (1.5 mM) was added to allow Ca^{2+} uptake into the stores, and when steady-state loading had been achieved, IP_3 was added with thapsigargin (1 μM) to allow Ca^{2+} release to be measured without further re-uptake. IP_3-evoked Ca^{2+} release is expressed as a fraction of the Ca^{2+} released by addition of ionomycin (1 μM) (12). Similar methods were used to measure IP_3-evoked Ca^{2+} release from Sf9 cells expressing IP_3R2.

Binding of ^{3}H-IP_3 to IP_3R2—Membranes were prepared from Sf9 cells expressing mouse IP_3R2 as described (17). Briefly, cells were harvested 60 h after infection, washed, and resuspended in Ca^{2+}-free CLM supplemented with complete protease inhibitor mixture (Roche Applied Science, 1 tablet/25 ml). The suspension (3×10^7 cells/ml) was homogenized and centrifuged (130,000 × *g*, 60 min), and the pellet was resuspended in Ca^{2+}-containing CLM and stored at −80 °C. Membranes (72 μg of protein/ml) were resuspended in CLM (0.5 ml, supplemented with 2 mM $MgCl_2$) containing [^{3}H]IP_3 (1.5 nM, 18 Ci/mmol) and appropriate concentrations of unlabeled IP_3. Variations in the composition of CLM at different steps were dictated by the need to minimize proteolysis during lysis (bivalent cation-free CLM) and then to include both Ca^{2+} and Mg^{2+} in the [^{3}H]binding assay more effectively to mimic the composition of cytosol and for comparison with our previous analyses of [^{3}H]IP_3 binding to IP_3R1 and IP_3R3 (16).

After 5 min at 2 °C, during which equilibrium was attained, the incubations were stopped by addition of γ-globulin (30 μl, 25 mg/ml) and polyethylene glycol 8000 (500 μl, 30%). After centrifugation (20,000 × *g* for 5 min at 2 °C), pellets were dissolved in Triton X-100 (200 μl, 2%), and ^{3}H activity was determined by liquid scintillation counting after addition of Ecoscint

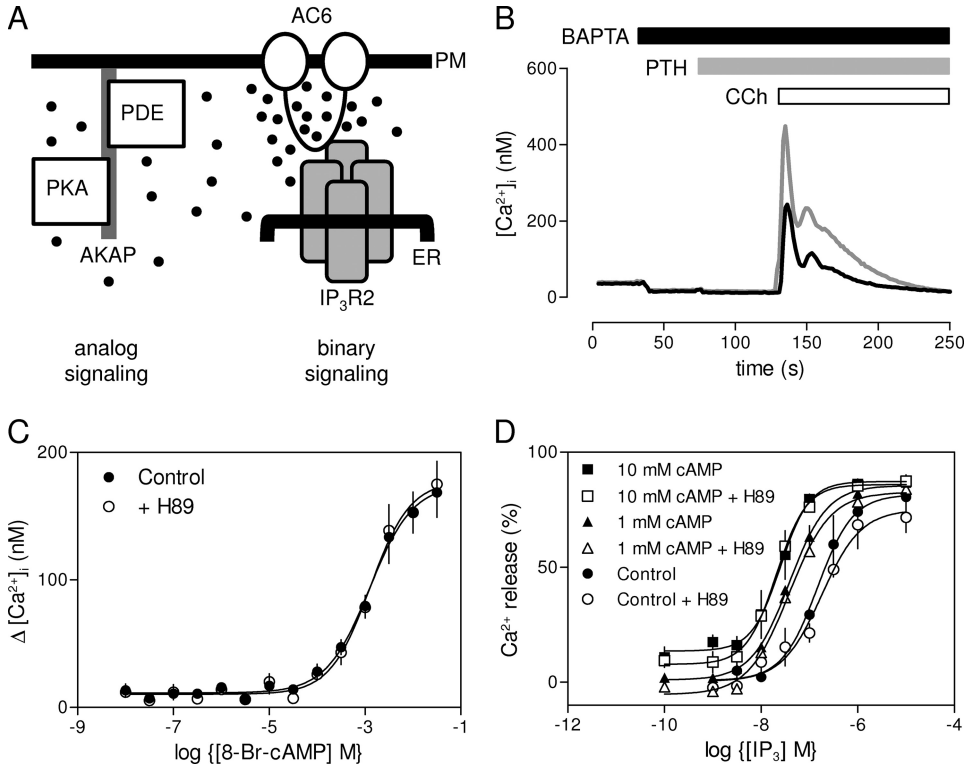

FIGURE 1. **PTH potentiates CCh-evoked Ca^{2+} release via a direct effect of cAMP on IP_3R.** *A*, binary and analog modes of cAMP signaling (7). *AKAP*, protein kinase A-anchoring protein; *PM*, plasma membrane. Further details are in text. *B*, populations of HEK-PR1 cells in Ca^{2+}-free HBS were stimulated with CCh alone (1 mM, *black line*) or with PTH (100 nM, 60 s) followed by CCh (*gray line*). Results are typical of at least three similar experiments. *C*, HEK-PR1 cells were preincubated (20 min) with the indicated concentrations of 8-Br-cAMP alone or with H89 (10 μM) (7) before stimulation with a submaximal concentration of CCh (1 μM). Results show the increase in $[Ca^{2+}]_i$ evoked by the CCh addition. *D*, IP_3-evoked Ca^{2+} release from permeabilized HEK-PR1 cells in the presence of submaximal (1 mM) or maximal (10 mM) concentrations of cAMP after preincubation with or without H89 (10 μM; 20 min). Results (*C* and *D*) show means ± S.E., $n = 3$ independent experiments.

A scintillation mixture (1 ml, National Diagnostics). Total $[^3H]IP_3$ binding was typically 2300 dpm, of which ~90% was specific binding. Results were fitted to Hill equations (GraphPad Prism, version 5) from which the half-maximal inhibitory concentration, and thereby the K_D, were determined.

Measurements of cAMP and $[Ca^{2+}]_i$ in Intact Cells—HEK-PR1 cells in 96-well plates were cultured for 2–3 days until almost confluent, washed, loaded with fluo-4, and $[Ca^{2+}]_i$ was then measured using a FlexStation fluorescence plate reader as described before (7). All experiments were performed at 20 °C in HBS or Ca^{2+}-free HBS. HBS had the following composition: 135 mM NaCl, 5.9 mM KCl, 1.2 mM $MgCl_2$, 1.5 mM $CaCl_2$, 11.6 mM HEPES, 11.5 mM glucose, pH 7.3; Ca^{2+}-free HBS was supplemented with 10 mM BAPTA.

Single cell analyses of $[Ca^{2+}]_i$ in fura-2-loaded HEK-PR1 cells were performed as previously reported, with fluorescence ratios calibrated, after correction for background fluorescence, to $[Ca^{2+}]_i$ by reference to Ca^{2+}-calibration solutions (18).

For assays of cAMP, HEK-PR1 cells in 24-well plates were cultured for 2–3 days (as above) until near confluence and then stimulated under identical conditions to those used for measurements of $[Ca^{2+}]_i$; the only difference was the omission of fluo-4-AM and Pluronic F-127 from the 1-h loading incubation. Cell extracts were prepared, and their cAMP content was determined by radioimmunoassay using acetylated standards prepared from a cAMP stock calibrated by its UV absorption (ϵ_{258} = 14,100) as described (7, 19). It is important to note that single cell measurements of $[Ca^{2+}]_i$ established that 98% of cells responded to CCh, and 99% of those responded to PTH (7). This observation justifies our use of cell populations for comparisons of the effects of stimuli on $[Ca^{2+}]_i$ and cAMP levels.

Nuclear Patch Clamp Recording—Currents were recorded from patches excised from the outer nuclear envelope of DT40-KO cells stably expressing mouse IP_3R2, using Cs^+ as the charge carrier. Bath and pipette (PS) solutions had the following composition: 200 mM $CsCH_3SO_3$, 500 μM BAPTA, 211 μM $CaCl_2$ (free $[Ca^{2+}]$ = 200 nM), 10 mM HEPES, pH 7.2 (with CsOH). Where appropriate, IP_3, cAMP, and/or ATP were included in PS. Data were collected and analyzed exactly as described previously (20).

Analysis—Concentration-effect relationships for each experiment were individually fitted to Hill equations using non-linear curve-fitting (GraphPad Prism, version 5), and the results obtained from each (EC_{50}, Hill coefficient h, and maximal response) were pooled for analysis and presentation. For simplicity, EC_{50} values are reported as means ± S.E., although log EC_{50} values were used for statistical analysis. Student's t test or one-way analysis of variance followed by post hoc Bonferroni test were used as appropriate.

Materials—Sources of materials not specified herein are provided in a previous study (7).

RESULTS AND DISCUSSION

Potentiation of IP_3-evoked Ca^{2+} Release by cAMP—CCh, which activates phospholipase C and thus IP_3 formation via endogenous muscarinic acetylcholine receptors, stimulated Ca^{2+} release from the intracellular stores of HEK-PR1 cells (Fig. 1*B*). The response was potentiated by forskolin, which activates AC directly (7), or by PTH, which activates AC via heterologously expressed type 1 PTH receptors and the G-protein, G_s (Fig. 1*B*). The effect of PTH on CCh-evoked Ca^{2+} release was mimicked by a membrane-permeant analogue of cAMP, 8-Br-cAMP (EC_{50} = 324 μM) (7), and the sensitivity to 8-Br-cAMP was unaffected by H89 at a concentration (10 μM) sufficient to inhibit fully PKA-mediated protein phosphorylation (Fig. 1*C*) (7). Neither forskolin nor 8-Br-cAMP alone evoked Ca^{2+} release (7).

In permeabilized HEK-PR1 cells, IP_3 stimulated release of Ca^{2+} from the intracellular stores, cAMP increased the sensi-

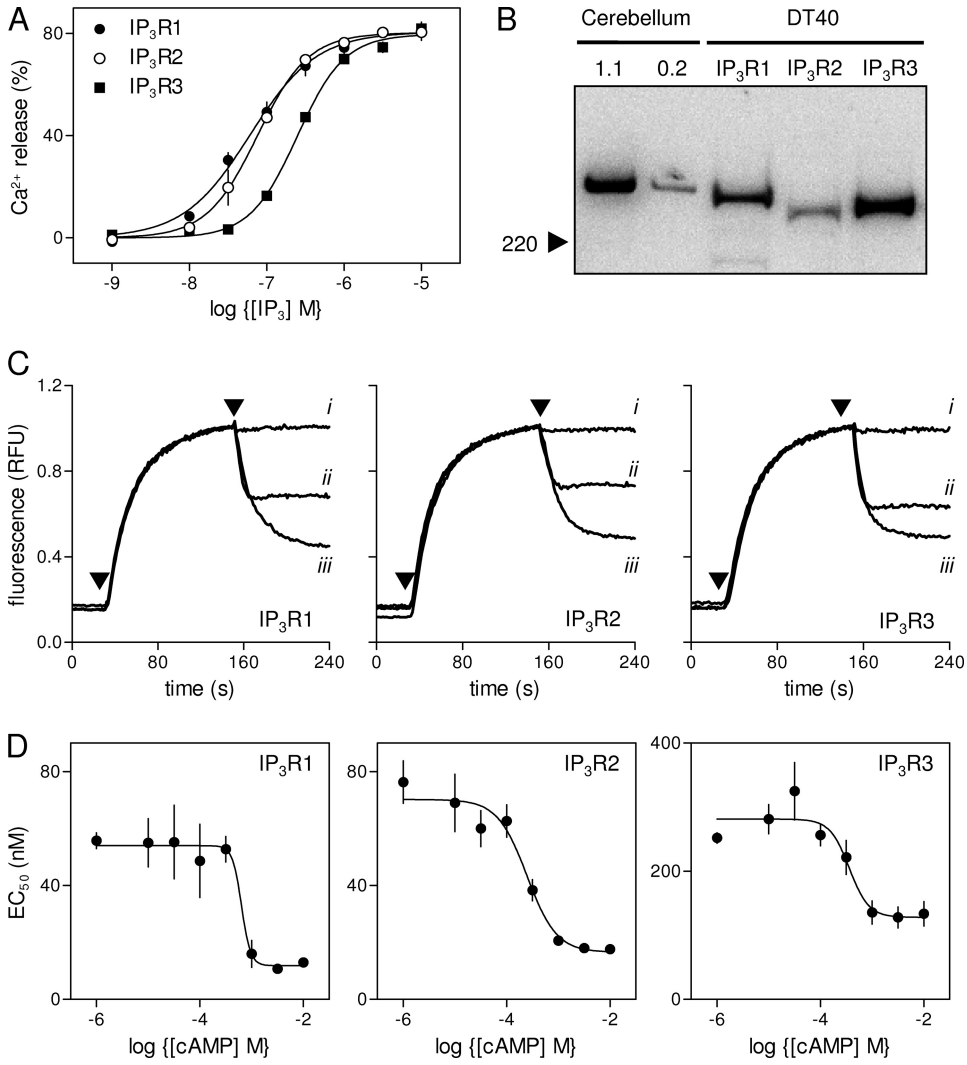

FIGURE 2. **cAMP potentiates IP_3-evoked Ca^{2+} release by the three subtypes of IP_3R.** *A*, IP_3-evoked Ca^{2+} release from the intracellular stores of DT40 cells expressing only IP_3R1, IP_3R2, or IP_3R3. *B*, immunoblots (with AbC) show levels of IP_3R expression in each of the three cell lines (95 μg of protein/*lane*) compared with membranes from rat cerebellum (1.1 and 0.2 μg/*lane*); the position of the 220-kDa M_r marker is shown. The blot is typical of six experiments from two different preparations. Summary results are shown in Table 1. *C*, typical results from permeabilized DT40 cells expressing the indicated IP_3R incubated with ATP (added at the *first arrow*) to allow loading of the intracellular Ca^{2+} stores, before addition (*second arrow*) of cAMP alone (*i*, 1 mM), IP_3 alone (*ii*, 30 nM for IP_3R1 and IP_3R2; 300 nM for IP_3R3), or IP_3 with cAMP (*iii*). Each *trace* is the average of three to four wells from a single experiment and is representative of results from three to four independent experiments. *D*, from experiments similar to those shown in *C*, the concentration-dependent effects of cAMP on the EC_{50} for IP_3-evoked Ca^{2+} release are shown for each IP_3R subtype. Results are means ± S.E., $n \geq 3$.

tivity to IP_3, and the effects of cAMP were again unaffected by inhibition of PKA (Fig. 1*D*). These results confirm our earlier conclusion that in HEK-PR1 cells, PTH potentiates IP_3-evoked Ca^{2+} release via cAMP and with no requirement for PKA (7). The earlier work established that IP_3R2 and AC6 are selectively associated and both are required for PTH to potentiate CCh-evoked Ca^{2+} signals (7) (Fig. 1*A*). But it is not yet clear whether the specific requirement for IP_3R2 derives entirely from its association with AC6 or is IP_3R2 also the only subtype of IP_3R to respond directly to cAMP?

Regulation of All IP_3R Subtypes by cAMP—IP_3 stimulated release of Ca^{2+} from the intracellular stores of permeabilized DT40 cells stably expressing mammalian IP_3R1, IP_3R2, or IP_3R3 (Fig. 2*A*), but not from the parental cells lacking endogenous IP_3R (not shown) (21, 22). Because the three IP_3R subtypes are not expressed at identical levels (Fig. 2*B* and Table 1), we cannot assume that the different fractions of the intracellular Ca^{2+} stores released by a maximal concentration of IP_3 or the different EC_{50} values (Table 1) directly reflect specific properties of the three IP_3R subtypes. It is generally suggested that IP_3R2 is more sensitive than IP_3R1 to IP_3, and both are considerably more sensitive than IP_3R3 (23, 24). However, in our assays of DT40 cells stably expressing a single IP_3R subtype we found the order of sensitivity to be: $IP_3R1 > IP_3R2 \gg IP_3R3$ (Table 1). The slightly lower than anticipated sensitivity of cells expressing IP_3R2 probably results from IP_3R2 being expressed at a lower level (~30–40%) than the other subtypes (Table 1) (21). The ~5-fold difference in IP_3 sensitivity between cells expressing IP_3R1 and IP_3R3 does not detract from our ability to resolve the effects of cAMP on IP_3-evoked Ca^{2+} release via each IP_3R subtype.

We used the three DT40 cell lines to examine the effects of cAMP on IP_3-evoked Ca^{2+} release. The results demonstrate that cAMP alone had no effect on the intracellular Ca^{2+} stores (Fig. 2*C*), but it significantly increased the sensitivity of each IP_3R subtype to IP_3 (Fig. 2, *C* and *D*). For all subtypes, a maximally effective concentration of cAMP caused the EC_{50} for IP_3-evoked Ca^{2+} release to decrease by between 2- and 4-fold (Table 1). This increase in sensitivity is similar to the ~3-fold increased sensitivity to CCh of HEK-PR1 cells treated with PTH (7), but less than the ~7-fold increase in IP_3 sensitivity evoked by a maximal concentration of cAMP in permeabilized HEK cells (Fig. 1*D*). There was no statistical difference ($p < 0.05$) between either the sensitivities of the three IP_3R subtypes to cAMP (EC_{50}) or the Hill coefficients of the concentration-effect relationships. We conclude that the three subtypes of IP_3R are similarly sensitive to cAMP, with EC_{50} values between ~300 and 650 μM (Table 1).

Interactions of cAMP with IP_3R2—Our earlier work established the importance of IP_3R2 in mediating responses to PTH (7) and responses of homomeric IP_3R2 are potentiated by cAMP (Fig. 2, *C* and *D*), we therefore focused on this IP_3R subtype for our further analyses of the interactions of cAMP with IP_3R.

TABLE 1

Responses of IP_3R subtypes to IP_3 and cAMP

Permeabilized DT40 cells expressing only a single mammalian IP_3R subtype were used to examine the sensitivity of the intracellular Ca^{2+} stores to IP_3 (EC_{50}) and the fraction of the stores released by a maximally effective concentration of IP_3. For each cell line, IP_3R expression was quantified using immunoblotting with AbC (Fig. 2*B*), which interacts equally with all three IP_3R subtypes (16) and calibrated against a stock of rat cerebellar membranes for which B_{max} (tetrameric $IP_3R/10^6$ cells) had been determined from [^{3}H]IP_3 binding. The effects of a maximally effective concentration of cAMP on the EC_{50} for IP_3-evoked Ca^{2+} release are shown, derived from experiments similar to those shown in Figs. 1*D* and 2. The sensitivity to cAMP is shown by the EC_{50} for the effects of cAMP on IP_3-evoked Ca^{2+} release. Results are means ± S.E. ($n \geq 3$).

	IP_3R1	IP_3R2	IP_3R3	IP_3R2-ΔATPB
IP_3R expression (fmol/10^6 cells)	38 ± 2	16 ± 1	56 ± 5	ND[a]
EC_{50} for IP_3 (nM)	56 ± 3	74 ± 10	255 ± 9	246 ± 17
EC_{50} for IP_3 after cAMP (nM)	13 ± 1	22 ± 1	134 ± 19	44 ± 3
Fold stimulation by cAMP	4.2 ± 0.1	3.3 ± 0.3	2.0 ± 0.3	5.7 ± 0.6
Maximum response to IP_3 (%)	83 ± 10	80 ± 1	80 ± 1	45 ± 4
Maximum response to IP_3 after cAMP (%)	79 ± 2	81 ± 1	82 ± 1	53 ± 4
EC_{50} for cAMP (μM)	642 ± 158	267 ± 80	361 ± 74	ND

[a] ND, not determined.

It proved impracticable to measure [^{3}H]IP_3 binding in CLM to membranes prepared from DT40-IP_3R2 cells; we therefore used membranes from Sf9 cells expressing the same mouse IP_3R2 (Fig. 3*A*). We first confirmed that IP_3R2 expressed in Sf9 cells are regulated by cAMP. Whereas IP_3 (10 μM) stimulated release of only 7 ± 1% (EC_{50} = 500 ± 50 nM) of the Ca^{2+} stores of uninfected Sf9 cells, it released 30 ± 4% (EC_{50} = 122 ± 35 nM) of the stores from permeabilized Sf9 cells expressing mouse IP_3R2 (Fig. 3*B*). This confirms that most IP_3-evoked Ca^{2+} release from the infected Sf9 cells is mediated by heterologously expressed IP_3R2. Treatment with cAMP (1 mM), which itself caused no Ca^{2+} release, increased the sensitivity of the expressed IP_3R2 to IP_3: the EC_{50} was reduced from 122 ± 35 nM to 41 ± 12 nM (Fig. 3*B*). These results establish that IP_3R2 expressed in Sf9 cells, like those expressed in HEK (7) or DT40 cells (Fig. 2), are sensitized to IP_3 by cAMP.

IP_3 bound to IP_3R2 expressed in Sf9 cells with high affinity (K_D = 4.30 ± 0.04 nM, B_{max} = 2.55 pmol/mg), but specific binding of [^{3}H]IP_3 (1.5 nM) was unaffected by cAMP (10 mM) (Fig. 3*C*). This demonstrates that the effect of cAMP on IP_3R2 is not mediated by an increase in its affinity for IP_3, but must instead result from an increase in the effectiveness with which IP_3 binding is coupled to channel opening; cAMP increases the efficacy of IP_3.

Effects of cAMP on Single IP_3R2—In patch clamp recordings from excised nuclear patches of DT40-IP_3R2 cells, IP_3 (100 μM) in the absence of ATP (which is not required for high concentrations of IP_3 to maximally activate IP_3R2 (25)) stimulated opening of large-conductance cation channels (γ_{Cs} ~200 pS, Fig. 4, *A*, *i*, and *ii*, and *B*). These channels were absent from the nuclei of DT40-KO cells (Fig. 4*A*, *iii*). The single channel open probability (P_o) of these IP_3R was similar (P_o = 0.49 ± 0.07) (Fig. 4*A*, *ii*) to that reported for maximally stimulated IP_3R2 expressed in the plasma membrane (25), or nuclear IP_3R1 and IP_3R3 (20). The latter recordings used K^+ as charge-carrier, but P_o for IP_3R1 is similar whether K^+ (P_o = 0.45 ± 0.07) or Cs^+ (P_o = 0.41 ± 0.04) is used as the charge carrier. These results establish that 100 μM IP_3 in the absence of ATP maximally activates IP_3R2.

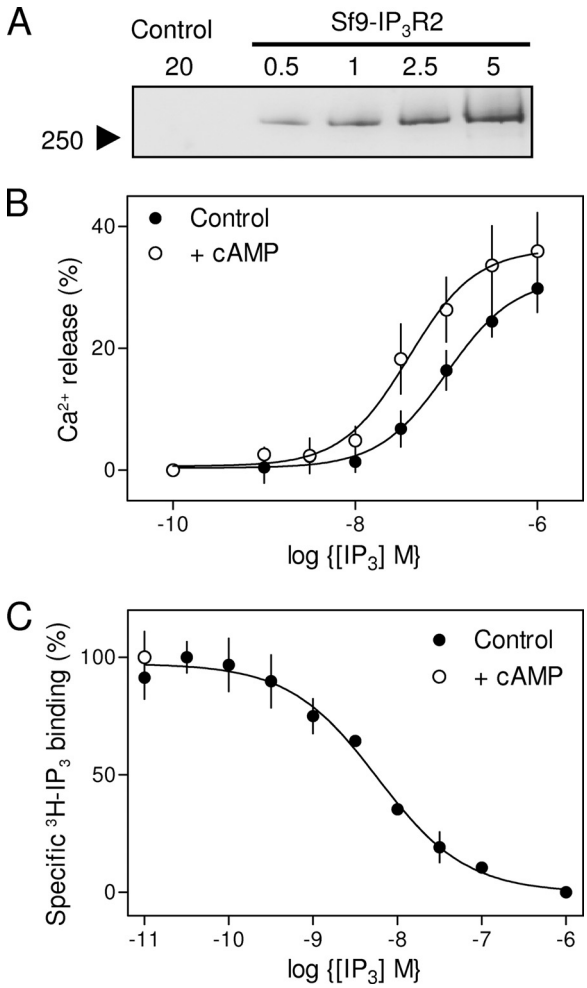

FIGURE 3. **Interaction of cAMP with IP_3R2 expressed in Sf9 cells.** *A*, immunoblot (with AbC) showing expression of IP_3R2 in membranes from infected Sf9 cells, but not from membranes of uninfected cells (control). Protein loadings are shown in micrograms. *B*, concentration-dependent release by IP_3 of Ca^{2+} from permeabilized Sf9 cells expressing mouse IP_3R2 with or without addition of cAMP (1 mM). *C*, specific binding of [^{3}H]IP_3 (1.5 nM) to membranes from Sf9 cells expressing mouse IP_3R2 in the presence of the indicated concentrations of unlabeled IP_3. There was no detectable specific binding of [^{3}H]IP_3 to membranes from uninfected cells. Because the concentration of [^{3}H]IP_3 (1.5 nM) was less than the K_D for IP_3 (4.3 nM), a change in K_D or B_{max} would be reflected in the specific [^{3}H]IP_3 binding. The *open circle* shows that cAMP (10 mM) had no effect on specific [^{3}H]IP_3 binding. Results (*B* and *C*) show means ± S.E., $n \geq 3$.

The effects of cAMP are most evident in Ca^{2+} release assays after submaximal activation with IP_3 (Fig. 1*D* and Table 1) (7). Our initial examination of the effects of cAMP on single IP_3R2 were therefore performed without ATP and with a submaximal concentration of IP_3. Because P_o is much lower under these conditions, it is impossible to resolve with confidence the number of active IP_3R within a patch (20) and so impossible to calculate P_o. We therefore use NP_o (the overall channel activity) to report the activity of IP_3R in these submaximally stimulated patches. A concentration of cAMP (1 mM) sufficient to sensitize maximally IP_3-evoked Ca^{2+} release (Fig. 2*D*) had no effect alone on channel activity recorded from nuclei of DT40-IP_3R2 cells (Fig. 4*C*, *i*). But cAMP significantly increased the activity of IP_3R2 stimulated with a submaximal concentration of IP_3 (1 μM): NP_o increased from 0.06 ± 0.02 (n = 11) in the absence of cAMP to 0.18 ± 0.05 (n = 5) in its presence (Fig. 4, *C*, *ii* and *iii*,

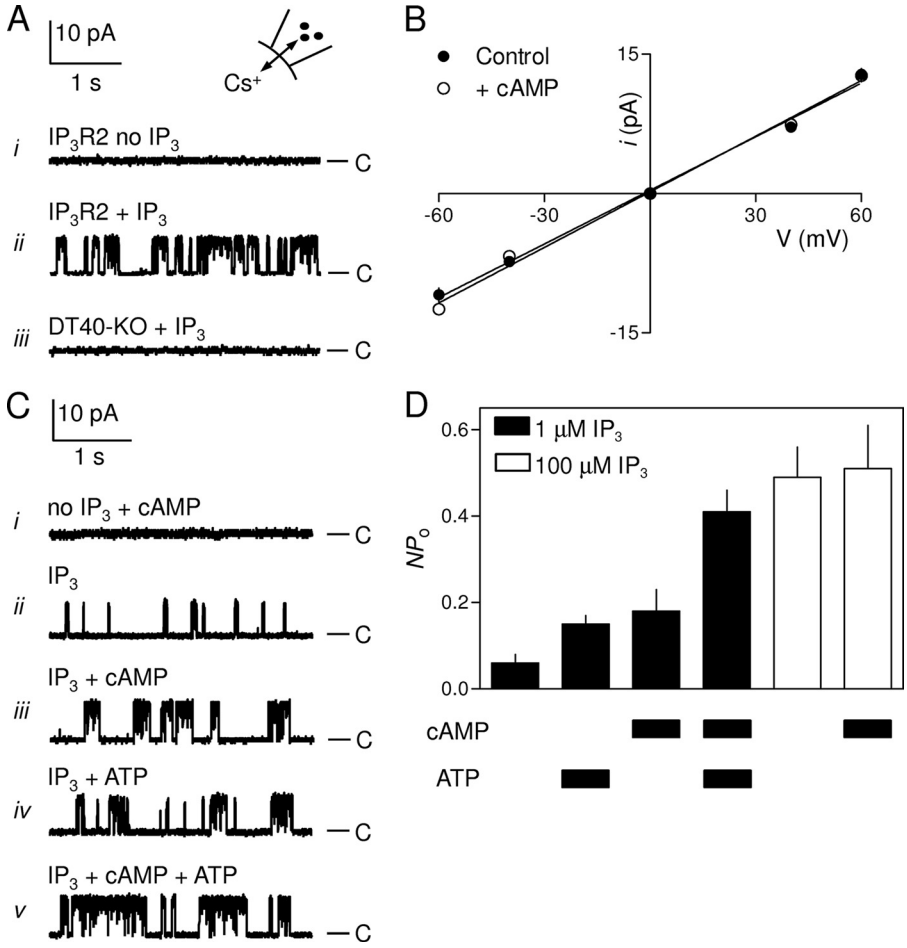

FIGURE 4. **Effects of cAMP on single channel activities of IP_3R2.** *A*, *traces* show excised nuclear patch clamp recordings from DT40-IP_3R2 (*i* and *ii*) or DT40-KO cells (*iii*) in which IP_3 (100 μM) was included in PS as indicated. *B*, current-voltage (*i-V*) relationship for single IP_3R2 stimulated with IP_3 (1 μM), with or without cAMP (1 mM) in PS. The single channel slope conductances (γ_{Cs}) were 204 ± 6 and 200 ± 12 pS in the absence and presence of cAMP, respectively. *C*, typical *traces* from single IP_3R2 stimulated with submaximal IP_3 (1 μM) in the presence and absence of cAMP (1 mM) and/or ATP (5 mM) in PS as indicated. *D*, from recordings similar to those shown in *D*, NP_o is shown for IP_3R2 stimulated as indicated. Note the use of NP_o to report channel activity here because the IP_3Rs are less active in some of the recording conditions, making it difficult to determine reliably the number of IP_3R in each patch (see text). For all *traces*, PS contained a free [Ca^{2+}] of 200 nM, the holding potential was +40 mV, *C* denotes the closed state, and each *trace* is typical of at least three similar recordings. Results (*B* and *D*) are means ± S.E., $n \geq 3$.

and *D*). The single channel Cs^+ conductance was unaffected by cAMP (Fig. 4*B*). Because these experiments were performed in the absence of ATP, the effects of cAMP cannot be attributed to PKA-mediated phosphorylation of IP_3R.

In keeping with work from others (25), ATP (5 mM) alone had no effect on IP_3R2 activity (not shown), but it potentiated responses to a submaximal concentration of IP_3 (1 μM): NP_o increased from 0.06 ± 0.02 ($n = 11$) to 0.15 ± 0.02 ($n = 5$) in the presence of ATP (Fig. 4, *C*, *ii*, and *iv*, and *D*). In the presence of this maximally effective concentration of ATP (25), cAMP (1 mM) further potentiated responses to IP_3 (1 μM): NP_o increased from 0.15 ± 0.02 to 0.41 ± 0.05 ($n = 6$) in the presence of cAMP (Fig. 4, *C*, *iv* and *v*, and *D*). In keeping with our results from Ca^{2+} release assays (Table 1), cAMP did not increase NP_o of IP_3R2 stimulated with a maximally effective concentration of IP_3 (100 μM): NP_o was 0.49 ± 0.07 and 0.51 ± 0.1 ($n = 3$) in the absence and presence of cAMP, respectively (Fig. 4*D*). We conclude that cAMP, either directly or via a tightly associated accessory protein, increases the activity of IP_3R2 stimulated with IP_3.

cAMP Potentiation of IP_3-evoked Ca^{2+} Release Is Not Mediated by the Modulatory ATP-binding Site—We further considered the possibility that the effects of cAMP might reflect its interaction with the site(s) through which ATP potentiates IP_3R function (25, 26). This seems unlikely from the results of our single channel analyses (Fig. 4) and because cAMP potentiates responses to IP_3 in the presence of 1.5 mM ATP (Fig. 2, *C* and *D*), which others have shown to be more than sufficient to potentiate maximally responses to IP_3 (25). Yule and coworkers have established that an ATP-binding site in IP_3R2 (ATPB, residues 1969–1974) mediates modulation of IP_3R2 gating by ATP. Mutation of glycine residues (G1969A, G1971A, and G1974A) within this site abolishes the potentiating effect of ATP on IP_3-evoked Ca^{2+} release (25). We used the same cell line (DT40-ΔATPB), kindly provided by David Yule (University of Rochester), to examine the effects of cAMP on IP_3-evoked Ca^{2+} release. Responses to IP_3 in these DT40-ΔATPB cells were also potentiated by cAMP (Fig. 5, *A* and *B*, and Table 1). These results, together with those from single channel analyses (Fig. 4), establish that the effects of cAMP on IP_3R2 are not mediated by its interaction with the site through which ATP potentiates activity.

PKA-dependent and -independent Regulation of IP_3R by cAMP—All three IP_3R subtypes respond directly to cAMP (Fig. 2), all three can also be phosphorylated, at multiple sites, by PKA (6, 7, 27–34), and substantial evidence suggests that the phosphorylation can modulate IP_3R activity (28, 31, 35–38). Phosphorylation of IP_3R1 by PKA increases their activity (27, 31, 32, 39–41). An initial suggestion that PKA inhibits IP_3R1 probably resulted from a counteracting stimulatory effect of PKA on Ca^{2+} re-uptake (30). IP_3R2 appears to be a rather poor substrate for PKA (7, 27, 28, 36), although it is phosphorylated at Ser-937 (34), and in cells expressing predominantly IP_3R2, PKA typically causes a very modest increase in their sensitivity to IP_3 (7, 28, 35, 42). In DT40 cells expressing only IP_3R2 forskolin enhances responses to IP_3, but the extent to which this requires activation of PKA is unclear. When a PKA-selective analog of cAMP was used, phosphorylation of Ser-937 by PKA was required for potentiation of the Ca^{2+} signals evoked by

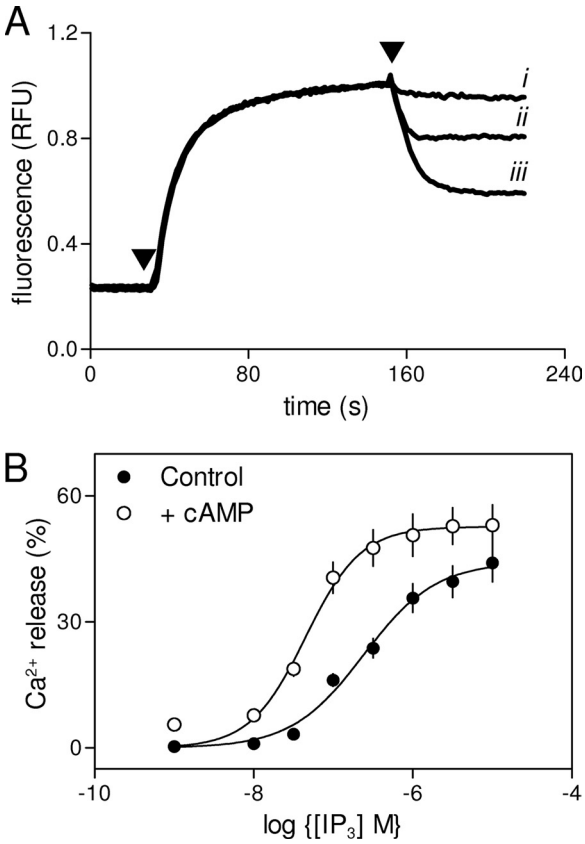

FIGURE 5. **Potentiation of IP_3R2 by cAMP does not require the ATPB-binding site.** *A*, typical results from permeabilized DT40 cells expressing only IP_3R2-ΔATPB incubated with ATP (added at the *first arrow*) before addition (*second arrow*) of cAMP alone (*i*, 3 mM), IP_3 alone (*ii*, 300 nM), or IP_3 with cAMP (*iii*). Each *trace* is the average of three to four wells from one experiment and is representative of results from three independent experiments. *B*, summary showing the concentration-dependent effects of IP_3 on Ca^{2+} release in the absence and presence of cAMP (3 mM). Results are means ± S.E., $n \geq 3$.

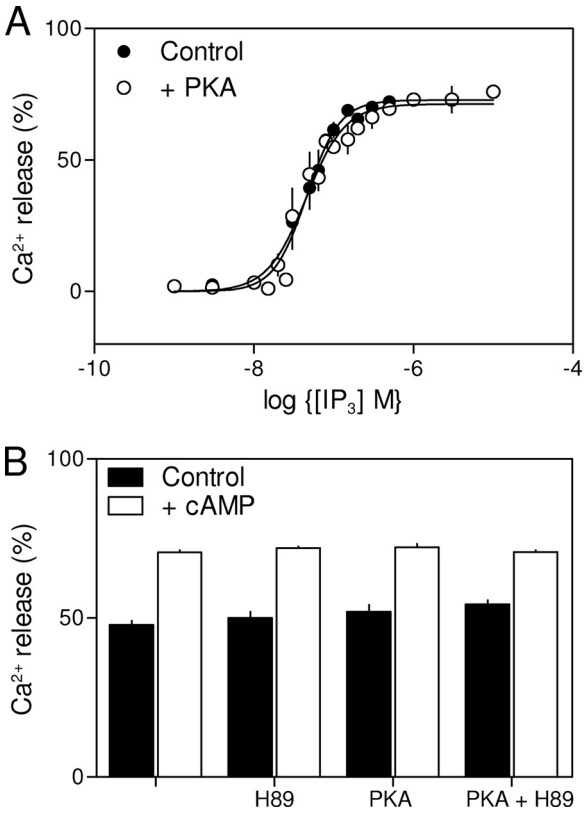

FIGURE 6. **Sensitization of IP_3R2 by cAMP does not require activation of PKA.** *A*, IP_3-evoked Ca^{2+} release from the intracellular stores of permeabilized DT40-IP_3R2 cells with and without preincubation with the catalytic subunit of PKA (200 units/ml, 10 min). *B*, Ca^{2+} release from permeabilized DT40-IP_3R2 cells stimulated with IP_3 alone (60 nM) or in combination with cAMP (3 mM) after the indicated pretreatments (10 min) with the catalytic subunit of PKA (200 units/ml) and/or H89 (10 μM). Results are means ± S.E., $n \geq 3$.

threshold concentrations of CCh (34). Clearly, therefore, PKA can both phosphorylate and modestly sensitize IP_3R2; the extent to which that underlies the effects of forskolin or cAMP is unresolved. The effects of PKA on IP_3R3 are less clear. Analyses from cells in which IP_3R3 is the major subtype suggest that PKA either modestly sensitizes them to IP_3 (28) or attenuates their responses (33, 43). The only published analysis of homomeric IP_3R3 expressed in DT40 cells concluded that PKA had no effect on IP_3-evoked Ca^{2+} release (27).

Under conditions where the catalytic subunit of PKA (200 units/ml for 10 min) phosphorylates IP_3R in HEK-PR1 cells (7), it had no effect on IP_3-evoked Ca^{2+} release from DT40 cells expressing IP_3R2 (Fig. 6*A*) or IP_3R3 (not shown), and it only very modestly increased the sensitivity of IP_3R1 to IP_3 (the EC_{50} fell from 36 to 27 nM (supplemental Fig. S1, *A* and *B*). We note that, even for IP_3R1, where the effects of PKA are relatively uncontentious, phosphorylation by PKA typically increases the IP_3 sensitivity by <2-fold (28, 36, 40). In our analyses of HEK-PR1 cells also, the very modest stimulatory effect of PKA on IP_3-evoked Ca^{2+} release (~30%) is much smaller than that of cAMP (~450%) (7).

In an attempt to reduce phosphorylation by endogenous PKA (41), we first incubated DT40-IP_3R2 cells with H89 (10 μM, 60 min) to inhibit PKA before permeabilizing the cells and assessing their responses to IP_3. Here too, there was no detectable effect of the catalytic subunit of PKA on IP_3-evoked Ca^{2+} release via IP_3R2 (supplemental Fig. S1*C*). Under the same conditions, where direct activation of PKA had no effect on IP_3-evoked Ca^{2+} release, cAMP (3 mM) potentiated the response to a submaximal concentration of IP_3 (60 nM) to the same extent whether applied alone, or after pretreatment (10 min) with H89 (10 μM), the catalytic subunit of PKA (200 units/ml) or both (Fig. 6*B*). We conclude that sensitization of IP_3R2 by cAMP occurs independently of activation of PKA.

We can only speculate on the negligible (IP_3R1) or undetectable effect (IP_3R2 and IP_3R3) of PKA on IP_3-evoked Ca^{2+} release from DT40 cells expressing homomeric IP_3R. Association of IP_3R with AKAP facilitates their phosphorylation by endogenous PKA (40, 44, 45), but ineffective targeting of PKA by AKAP is unlikely to prevent exogenous catalytic subunit of PKA from phosphorylating IP_3R (Fig. 6 and supplemental Fig. S1). Accessory proteins, perhaps analogous to the IP_3R-associated cGMP kinase substrate (IRAG) required for regulation of IP_3R by cGMP-dependent protein kinase (46), may be required for PKA to modulate IP_3R activity. IP_3R may already be phosphorylated in DT40 cells, although the lack of effect of PKA in permeabilized cells after sustained pretreatment of intact cells with an inhibitor of PKA suggests this is unlikely (supplemental Fig. S1*C*). Furthermore, even when IP_3R3 was shown to be phosphorylated by PKA in DT40 cells,

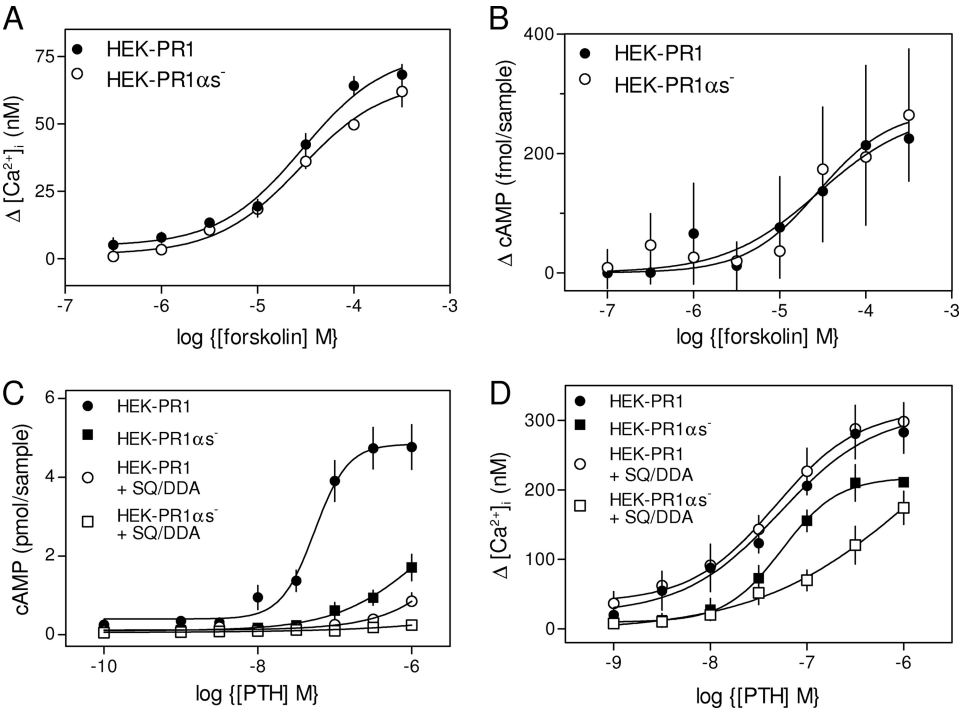

FIGURE 7. **Loss of $G\alpha_s$ attenuates PTH-potentiated Ca^{2+} signals.** *A* and *B*, concentration-dependent effects of forskolin on the potentiation of the Ca^{2+} release evoked by CCh (1 mM) (*A*) and on the increase in cAMP production measured 30 s after stimulation of HEK-PR1 and HEK-PR1α_s^- cells (*B*). *C*, concentration-dependent effects of PTH on cAMP formation (measured after 30 s) in HEK-PR1 and HEK-PR1α_s^- cells alone or after pre-incubation (20 min) with SQ 22536 (SQ, 1 mM) and 2′,5′-dideoxyadenosine (DDA, 200 μM) (SQ/DDA). *D*, cells treated as in *C* (with the same *symbols*) but showing the effects of PTH on CCh-evoked Ca^{2+} signals. Results (*A–D*) are means ± S.E., $n \geq 3$.

TABLE 2

Potentiation of CCh-evoked Ca^{2+} signals by PTH in $G\alpha_s$-deficient cells

The EC_{50} values for potentiation of CCh-evoked Ca^{2+} release by PTH or forskolin in populations of HEK-PR1 cells are shown. Results are means ± S.E., $n \geq 3$. Single cells loaded with fura-2 were stimulated with CCh alone (1 mM) followed by PTH (100 nM) in the continued presence of CCh. Responses from 6–12 independent coverslips, each including 116–233 cells, were analyzed. The results show the increase in $[Ca^{2+}]_i$ and the fraction of responsive cells in HEK-PR1 and HEK-PR1α_s^- cells.

	HEK-PR1	HEK-PR1α_s^-
Cell populations		
PTH	52 ± 10 nM	62 ± 11 nM[a]
PTH + H89	ND[b]	46 ± 12 nM
PTH + SQ/DDA	ND[b]	219 ± 27 nM[a]
Forskolin	30 ± 6 μM	28 ± 5 μM
Single cells		
Initial response to CCh, $\Delta[Ca^{2+}]_i$	585 ± 17 nM	593 ± 13 nM
PTH then CCh, $\Delta[Ca^{2+}]_i$	257 ± 32 nM[c]	183 ± 11 nM[c]
Cells responding to PTH then CCh	95 ± 1%	91 ± 3%

[a] $p < 0.05$ (between marked values).
[b] ND, not determined.
[c] $p < 0.05$ (between marked values).

there was no change in their response to IP_3 (27). A further possibility is that an active protein phosphatase is associated with IP_3R (32, 47) and limits their steady-state phosphorylation in DT40 cells.

The essential point for the present discussion is that cAMP directly potentiates IP_3-evoked Ca^{2+} release and the effect is both more substantial than, and independent of, the effects of phosphorylation by PKA.

Loss of $G\alpha_s$ Attenuates Sensitization of IP_3 Receptors by PTH—Potentiation of CCh-evoked Ca^{2+} signals by forskolin or PTH requires an intimate association between IP_3R2 and AC6 that allows cAMP to pass directly to the IP_3R (7) (Fig. 1*A*). Subsequent experiments seek to establish whether $G\alpha_s$, which links PTH receptors to activation of AC, is also specifically associated with these AC·IP_3R junctions.

We established seven stable HEK-PR1 cell lines in which shRNA was used to reduce expression of $G\alpha_s$ (HEK-PR1α_s^- cells) and three mock transfected lines. The responses of the latter to CCh alone or with PTH were indistinguishable from the parental cells (not shown). Results are shown for only one of the HEK-PR1α_s^- lines, in which $G\alpha_s$ expression was reduced by >95% (7). The concentration-dependent effects of CCh alone or with PTH on Ca^{2+} signals were similar in each of the other HEK-PR1α_s^- lines. Neither the Ca^{2+} signals evoked by CCh alone (7), their potentiation by forskolin (Fig. 7*A*), nor forskolin-stimulated cAMP production (Fig. 7*B*) was affected by loss of $G\alpha_s$. This establishes that selection of the stable HEK-PR1α_s^- cells had no effect on AC activity, CCh-mediated Ca^{2+} signaling, or potentiation of IP_3R activity by cAMP.

To allow direct comparison between PTH-evoked Ca^{2+} and cAMP signals, we measured both responses under the same conditions, after identical intervals (30 s) and in the absence of 3-isobutylmethylxanthine (see "Experimental Procedures"). Under these conditions, PTH caused a concentration-dependent stimulation of AC activity in both HEK-PR1 and HEK-PR1α_s^- cells (Fig. 7*C*). Loss of $G\alpha_s$ caused the EC_{50} for PTH-evoked cAMP formation to increase by at least 10-fold (Fig. 7*C*), while the maximal response (to 1 μM PTH) was reduced by 61 ± 7% and then reduced further (by 90 ± 5%) when AC was inhibited by SQ 22536 (1 mM) with DDA (200 μM) (SQ/DDA). In HEK-PR1 cells, inhibition of AC by SQ/DDA more fully inhibited PTH-evoked cAMP formation (81 ± 5%) than did loss of $G\alpha_s$ (61 ± 7%) (Fig. 7*C*).

Inhibition of AC alone had no effect on PTH-potentiated Ca^{2+} signals (Fig. 7*D*) (7), but loss of $G\alpha_s$ reduced their peak amplitude without affecting their sensitivity to PTH (Fig. 7*D* and Table 2). We confirmed, using single cell analyses of $[Ca^{2+}]_i$, that the same fraction of cells responded to PTH in normal and $G\alpha_s$-deficient cells, that the two cell lines responded similarly to CCh alone, and that the amplitude of the PTH-potentiated CCh-evoked Ca^{2+} signal was decreased by 29 ± 4% in HEK-PR1α_s^- cells (Table 2). This demonstrates that the results with cell populations, where loss of $G\alpha_s$ diminished peak PTH-evoked Ca^{2+} signals by 34 ± 3% (Fig. 7*D*), do not arise from an all-or-nothing loss of

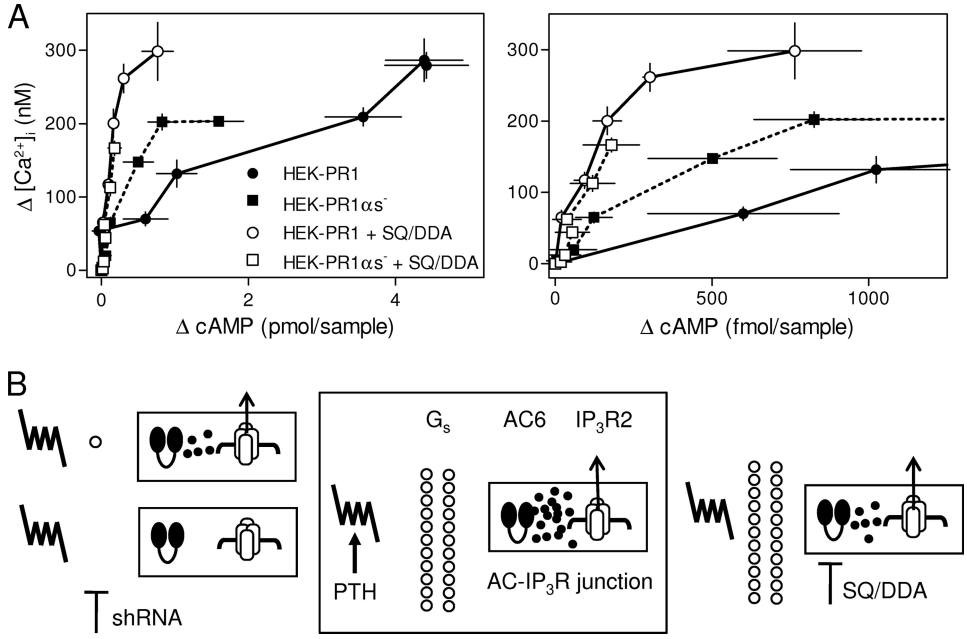

FIGURE 8. **Association of $G\alpha_s$ with AC·IP_3R junctions.** *A*, from the results shown in Fig. 7, *C* and *D*, the relationships between the change in cAMP content and potentiation of CCh-evoked Ca^{2+} signals by PTH are shown for HEK-PR1 and HEK-PR1α_s^- cells alone or after pretreatment with SQ/DDA (20 min). The *right panel* shows an enlarged version of the relationship for the lower ΔcAMP levels. Results are means ± S.E., $n \geq 3$. *B*, proposed arrangement of AC·IP_3R junctions. The *central panel* shows the signaling proteins that regulate the AC·IP_3R junction, allowing AC6 to deliver super-saturating concentrations of cAMP to an associated IP_3R2. The predicted consequences of incompletely inhibiting AC with low affinity inhibitors (SQ/DDA, *right*) or diminishing AC activity by removal of $G\alpha_s$ from AC·IP_3R junctions (shRNA, *left*) are shown. As long as some $G\alpha_s$ remains associated with the junction, the cAMP safety margin allows effective signaling to the IP_3R (*upper left*), but complete removal of $G\alpha_s$ from a junction incapacitates signaling (*lower left*). We speculate that ~22 $G\alpha_s$ associate with each AC·IP_3R junction (see text). Whether PTH receptors associate specifically with individual junctions has not yet been addressed.

responsiveness of individual cells. For each cell, therefore, loss of >95% of $G\alpha_s$ caused a ~30% decrease in the peak Ca^{2+} signals evoked by PTH.

These results establish that the ability of all concentrations of PTH to potentiate CCh-evoked Ca^{2+} signals is insensitive to a uniform ~80% inhibition of AC activity by low affinity inhibitors of AC (SQ/DDA). But a lesser inhibition of AC arising from loss of $G\alpha_s$ attenuates PTH-mediated Ca^{2+} signaling (Fig. 7*D*). Why should inhibition of AC activity by loss of $G\alpha_s$ more effectively inhibit PTH-mediated Ca^{2+} signaling than direct inhibition of AC by low affinity inhibitors?

Association of $G\alpha_s$ with AC·IP_3R Junctions—Earlier experiments comparing the effects of inhibiting AC by reducing its expression with RNA interference or by inhibition of AC with SQ/DDA revealed a similar phenomenon to that observed with loss of $G\alpha_s$. Complete inhibition of AC within individual AC·IP_3R junctions by selective inhibition of AC6 expression attenuated PTH-evoked Ca^{2+} signaling. However, a greater, but uniformly distributed, inhibition by low affinity inhibitors of AC (SQ/DDA) had no effect on Ca^{2+} signaling (7). These and related results lead to our conclusion that the AC·IP_3R junction (Fig. 1*A*) is the minimal signaling unit and that within it cAMP is delivered to IP_3R at concentrations greater than are needed maximally to sensitize associated IP_3R. Each junction operates with a substantial "safety margin." Removing AC from individual junctions (by inhibition of AC expression) incapacitates individual junctions, whereas SQ/DDA uniformly attenuates cAMP formation at each junction, but the lesser amount of cAMP made within each is still sufficient to sustain effective communication between AC and IP_3R (7).

Attenuation of the responses to PTH by loss of $G\alpha_s$ might result entirely from the diminished activity of AC, or it might reflect an additional stimulatory role for Gs in modulating responses of IP_3R to cAMP. We previously demonstrated that the maximal effects of 8-Br-cAMP and PTH on the sensitivity of Ca^{2+} release to CCh were the same, and the two stimuli together had no greater effect (7). This provided persuasive evidence that cAMP alone mediates the effects of PTH on IP_3R sensitivity. That conclusion is further supported by the results shown in Fig. 8*A*, in which we compare the amounts of cAMP associated with comparable Ca^{2+} signals evoked by PTH under different conditions. The comparison is reasonable, because cAMP and $[Ca^{2+}]_i$ are measured at the same time (30 s) under identical conditions, and single cell analyses confirm that all cells respond similarly (Table 2). Comparably potentiated Ca^{2+} signals are associated with larger amounts of cAMP in normal HEK-PR1 cells than in HEK-PR1α_s^- cells. These results, where cells with most $G\alpha_s$ appear least sensitive to cAMP, are inconsistent with $G\alpha_s$ potentiating the responses of IP_3R to cAMP. These results reinforce our initial conclusion that cAMP alone mediates the effects of PTH on IP_3R (7).

Although cAMP is the only signal through which PTH communicates with IP_3R, the effective cAMP cannot be uniformly distributed, because otherwise the effects of inhibiting cAMP formation should be identical whatever step in the signaling pathway is targeted for inhibition. We speculate that a small number of $G\alpha_s$ are specifically associated with each AC·IP_3R junction (Fig. 8*B*). Random removal of $G\alpha_s$ from the signaling complex (by inhibition of $G\alpha_s$ expression) inactivates signaling from PTH to a complex without $G\alpha_s$, whereas complexes with residual $G\alpha_s$ continue to function, albeit with a lesser cAMP "safety margin" (Fig. 8*B*, *upper left*) than normal junctions. Hence, for HEK-PR1α_s^- cells, PTH-potentiated Ca^{2+} signals are associated with lesser overall increases in cAMP than in HEK-PR1 cells (Fig. 8*A*). The maximal potentiated Ca^{2+} signal evoked by PTH is decreased by 30% in HEK-PR1α_s^- cells, even though lesser amounts of cAMP in normal cells with AC inhibited by SQ/DDA are associated with undiminished Ca^{2+} signals (Fig. 7*D*). These results suggest that the ≥95% knockdown of $G\alpha_s$ inactivates signaling by PTH to ~30% of the AC·IP_3R

junctions. Assuming that a single $G\alpha_s$ is sufficient to mediate effective transmission to an AC·IP_3R junction and that the 95% loss of $G\alpha_s$ is randomly distributed among the junctions, we predict (supplemental text) that there is an average of 1.1 $G\alpha_s$ within each functional synapse of $G\alpha_s$-deficient cells, and ~22 $G\alpha_s$/synapse in normal cells.

Conclusions: Structure and Function of AC·IP_3R Junctions—We have shown that all three IP_3R subtypes are directly regulated by cAMP binding either directly to the IP_3R or to a protein tightly associated with it (Figs. 1–4). The effect of cAMP, which increased the efficacy of IP_3 (Fig. 4), required neither PKA (Fig. 6) nor the site through which ATP modulated IP_3R2 activity (Figs. 4 and 5). In HEK cells, we have established that a specific association of IP_3R2 with AC6 allows cAMP to pass directly from AC to the IP_3R within an AC·IP_3R junction (Fig. 8*B*) (7). This "binary mode" of cAMP signaling (Fig. 1*A*) allows robust communication between cell surface receptors and IP_3R, because each AC·IP_3R junction operates as an on-off switch with a large safety margin. The similar sensitivity of all IP_3R to cAMP (Fig. 2) suggests that the specific requirement for IP_3R2 in HEK cells derives from IP_3R2 selectively associating with AC6 to form the junctions required to deliver cAMP at sufficient concentration to regulate IP_3R. Results from cells with much reduced expression of $G\alpha_s$ (Figs. 7 and 8) suggest that small numbers of $G\alpha_s$ (~22 α_s/AC·IP_3R junction) may also associate with the AC·IP_3R junction (Fig. 8*B*).

IP_3 and cAMP are ubiquitous intracellular messengers, and interactions between them are common. Here we demonstrate another level of interaction in which cAMP itself sensitizes each IP_3R subtype by increasing the efficacy of IP_3. The interaction is not mediated by PKA, nor does it involve the ATP-binding site of the IP_3R. It remains to be resolved whether cAMP binds directly to IP_3R or to a tightly associated accessory protein. Within intact HEK cells, a selective association of IP_3R2 with AC6 to form an AC·IP_3R junction (Fig. 1*A*) allows cAMP preferentially to regulate IP_3R2. The G-protein, G_s, that couples PTH to stimulation of AC, appears also to selectively associate with the AC·IP_3R signaling junction. Aside from defining a novel interaction between cAMP and Ca^{2+} signaling pathways, our results highlight the importance of the spatial organization of both pathways in mediating effective signal transduction.

Acknowledgments—We thank Dr. F. Wolfram (Cambridge) for completing preliminary functional analyses of Sf9 cells, and Drs. D. Yule (Rochester) and K. Mikoshiba (Tokyo) for kind gifts of DT40ΔATPB cells and plasmid encoding mouse IP_3R2, respectively.

REFERENCES

1. Berridge, M. J., Lipp, P., and Bootman, M. D. (2000) *Nat. Rev. Mol. Cell Biol.* **1,** 11–21
2. Willoughby, D., and Cooper, D. M. (2007) *Physiol. Rev.* **87,** 965–1010
3. Zaccolo, M., Di Benedetto, G., Lissandron, V., Mancuso, L., Terrin, A., and Zamparo, I. (2006) *Biochem. Soc. Trans.* **34,** 495–497
4. Scott, J. D., and Pawson, T. (2009) *Science* **326,** 1220–1224
5. Werry, T. D., Wilkinson, G. F., and Willars, G. B. (2003) *Biochem. J.* **374,** 281–296
6. Bruce, J. I., Straub, S. V., and Yule, D. I. (2003) *Cell Calcium* **34,** 431–444
7. Tovey, S. C., Dedos, S. G., Taylor, E. J., Church, J. E., and Taylor, C. W. (2008) *J. Cell Biol.* **183,** 297–311
8. Mongillo, M., Tocchetti, C. G., Terrin, A., Lissandron, V., Cheung, Y. F., Dostmann, W. R., Pozzan, T., Kass, D. A., Paolocci, N., Houslay, M. D., and Zaccolo, M. (2006) *Circ. Res.* **98,** 226–234
9. Short, A. D., and Taylor, C. W. (2000) *J. Biol. Chem.* **275,** 1807–1813
10. Brummelkamp, T. R., Bernards, R., and Agami, R. (2002) *Science* **296,** 550–553
11. Sugawara, H., Kurosaki, M., Takata, M., and Kurosaki, T. (1997) *EMBO J.* **16,** 3078–3088
12. Tovey, S. C., Sun, Y., and Taylor, C. W. (2006) *Nat. Protoc.* **1,** 259–263
13. Mignery, G. A., Newton, C. L., Archer, B. T., 3rd, and Südhof, T. C. (1990) *J. Biol. Chem.* **265,** 12679–12685
14. Iwai, M., Tateishi, Y., Hattori, M., Mizutani, A., Nakamura, T., Futatsugi, A., Inoue, T., Furuichi, T., Michikawa, T., and Mikoshiba, K. (2005) *J. Biol. Chem.* **280,** 10305–10317
15. Blondel, O., Takeda, J., Janssen, H., Seino, S., and Bell, G. I. (1993) *J. Biol. Chem.* **268,** 11356–11363
16. Cardy, T. J., Traynor, D., and Taylor, C. W. (1997) *Biochem. J.* **328,** 785–793
17. Nerou, E. P., Riley, A. M., Potter, B. V., and Taylor, C. W. (2001) *Biochem. J.* **355,** 59–69
18. Tovey, S. C., Goraya, T. A., and Taylor, C. W. (2003) *Br. J. Pharmacol.* **138,** 81–90
19. Brooker, G., Harper, J. F., Terasaki, W. L., and Moylan, R. D. (1979) *Adv. Cyclic Nucleotide Res.* **10,** 1–33
20. Taufiq-Ur-Rahman, Skupin, A., Falcke, M., and Taylor, C. W. (2009) *Nature* **458,** 655–659
21. Dellis, O., Dedos, S. G., Tovey, S. C., Taufiq-Ur-Rahman, Dubel, S. J., and Taylor, C. W. (2006) *Science* **313,** 229–233
22. Sun, Y., and Taylor, C. W. (2008) *Biochem. J.* **416,** 243–253
23. Tu, H., Wang, Z., Nosyreva, E., De Smedt, H., and Bezprozvanny, I. (2005) *Biophys. J.* **88,** 1046–1055
24. Iwai, M., Michikawa, T., Bosanac, I., Ikura, M., and Mikoshiba, K. (2007) *J. Biol. Chem.* **282,** 12755–12764
25. Betzenhauser, M. J., Wagner, L. E., 2nd, Iwai, M., Michikawa, T., Mikoshiba, K., and Yule, D. I. (2008) *J. Biol. Chem.* **283,** 21579–21587
26. Bezprozvanny, I., and Ehrlich, B. E. (1993) *Neuron* **10,** 1175–1184
27. Soulsby, M. D., and Wojcikiewicz, R. J. (2007) *Cell Calcium* **42,** 261–270
28. Wojcikiewicz, R. J., and Luo, S. G. (1998) *J. Biol. Chem.* **273,** 5670–5677
29. Soulsby, M. D., and Wojcikiewicz, R. J. (2005) *Biochem. J.* **392,** 493–497
30. Supattapone, S., Danoff, S. K., Theibert, A., Joseph, S. K., Steiner, J., and Snyder, S. H. (1988) *Proc. Natl. Acad. Sci. U.S.A.* **85,** 8747–8750
31. Nakade, S., Rhee, S. K., Hamanaka, H., and Mikoshiba, K. (1994) *J. Biol. Chem.* **269,** 6735–6742
32. Tang, T. S., Tu, H., Wang, Z., and Bezprozvanny, I. (2003) *J. Neurosci.* **23,** 403–415
33. Giovannucci, D. R., Groblewski, G. E., Sneyd, J., and Yule, D. I. (2000) *J. Biol. Chem.* **275,** 33704–33711
34. Betzenhauser, M. J., Fike, J. L., Wagner, L. E., 2nd, and Yule, D. I. (2009) *J. Biol. Chem.* **284,** 25116–25125
35. Burgess, G. M., Bird, G. S., Obie, J. F., and Putney, J. W., Jr. (1991) *J. Biol. Chem.* **266,** 4772–4781
36. Dyer, J. L., Mobasheri, H., Lea, E. J., Dawson, A. P., and Michelangeli, F. (2003) *Biochem. Biophys. Res. Commun.* **302,** 121–126
37. Quinton, T. M., and Dean, W. L. (1992) *Biochem. Biophys. Res. Commun.* **184,** 893–899
38. DeSouza, N., Reiken, S., Ondrias, K., Yang, Y. M., Matkovich, S., and Marks, A. R. (2002) *J. Biol. Chem.* **277,** 39397–39400
39. Wagner, L. E., 2nd, Li, W. H., Joseph, S. K., and Yule, D. I. (2004) *J. Biol. Chem.* **279,** 46242–46252
40. Wagner, L. E., 2nd, Li, W. H., and Yule, D. I. (2003) *J. Biol. Chem.* **278,** 45811–45817
41. Wagner, L. E., 2nd, Joseph, S. K., and Yule, D. I. (2008) *J. Physiol.* **586,** 3577–3596

42. Bruce, J. I., Shuttleworth, T. J., Giovannucci, D. R., and Yule, D. I. (2002) *J. Biol. Chem.* **277,** 1340–1348
43. LeBeau, A. P., Yule, D. I., Groblewski, G. E., and Sneyd, J. (1999) *J. Gen. Physiol.* **113,** 851–872
44. Tu, H., Tang, T. S., Wang, Z., and Bezprozvanny, I. (2004) *J. Biol. Chem.* **279,** 19375–19382
45. Collado-Hilly, M., and Coquil, J. F. (2009) *Biol. Cell* **101,** 469–480
46. Schlossmann, J., Ammendola, A., Ashman, K., Zong, X., Huber, A., Neubauer, G., Wang, G. X., Allescher, H. D., Korth, M., Wilm, M., Hofmann, F., and Ruth, P. (2000) *Nature* **404,** 197–201
47. Cameron, A. M., Steiner, J. P., Roskams, A. J., Ali, S. M., Ronnett, G. V., and Snyder, S. H. (1995) *Cell* **83,** 463–472